An Experimental Study of the Effect of Gravity on Foam in Fractures

Li, K.; Wolf, K.H.A.A.; Rossen, W.R.

DOI
10.3997/2214-4609.202011063

Publication date
2020

Document Version
Accepted author manuscript

Published in
82nd EAGE Conference & Exhibition 2020

Introduction

Gas-injection EOR processes usually have poor sweep efficiency due to conformance problems including channelling, gravity override and viscous fingering. Conformance problems happen because the reservoir formation is heterogeneous, and displacing gas has lower density and viscosity compared to reservoir fluids. Naturally Fractured Reservoirs (NFRs) gain much attention worldwide because of their large reserves of hydrocarbons. However in NFRs, sweep efficiency of gas injection is further jeopardized, because of large difference of permeability in matrix and fractures. As a result, gas breaks through fractures first, leaving most oil behind in the matrix.

Foam EOR, created by adding surfactant solution in gas injection, can solve conformance problems and hence improve sweep efficiency. Strong foam can also be created in fractures (Kovscek et al., 1995; AlQuaimi and Rossen, 2019), thus building up a viscous pressure drop and diverting the flow of gas into matrix, and hence increasing the oil recovery (Farajzadeh et al., 2012).

In the field, fractures are by nature vertically oriented, because the original least principal stress is in horizontal direction in most formations. Foam performance in fractured reservoirs is affected not only by fracture roughness, aperture, etc., but also by gravity. Understanding how gravity affects the stability of foam is imperative for a successful foam application in fractured reservoirs.

In this study, we investigate how gravity affects foam in fractures. To this end, we have conducted seven sets of foam-scan experiments (i.e., a set of constant-total-velocity experiments, each with a different gas fractional flow) on three glass model fractures (model A, model B and model C) with hydraulic aperture of 78, 98 and 128 μm respectively. We compare the behaviour of foam in the models placed horizontally and vertically.

Experimental Apparatus and Materials

The experimental setup in this study is shown in Figure 1. A pump (VINDUM Engineering, model VP1-12K) is used to inject surfactant solution. A mass flow controller (Bronkhorst Nederland BV, F-230M) is used to inject gas. Seven absolute pressure transducers (DEMO MPXH6400A, 4 bar) are used to measure pressure at different locations along the model fracture.

Three models (model A, model B and model C) are used in this study. They have the same dimensions of 1 m x 0.15 m (L x W) and the same fracture roughness pattern. The hydraulic apertures, d_h, of three models are 78, 98 and 128 μm, respectively. Each model fracture is made of two glass plates, including one smooth plate and one single-side-rough plate (AlQuaimi and Rossen, 2019). The thickness of both plates is 20 mm.

The two plates are glued together along four edges to make the model fracture. Then the model is put into an aluminium clamping frame (Figure 2). The space between the two plates represents fracture aperture. The rough side of single-side-rough plate models the asperities of fracture wall. In total 11 holes are drilled through the rough plate for foam injection, production and connection to the pressure transducers. Two troughs with dimensions of 10 x 1 x 0.04 cm (L x W x H) are milled on the rough plate.

The glass models are transparent, hence allowing a direct investigation of foam texture inside the fracture using a high-speed camera (Photron Fastcam UX50). A high-parallelism chip back-light device (VAL LED lighting, VL-CB-CL) is used to provide light for the camera. The whole setup is placed inside a light-preventing tent to avoid external reflections and to improve the quality of images.

All experiments in this study are carried out at 20°C and ambient pressure. Nitrogen is the gas phase, and surfactant solution is 1 wt % AOS C14-16 (Stepan® BIO-TERGE AS-40 KSB).

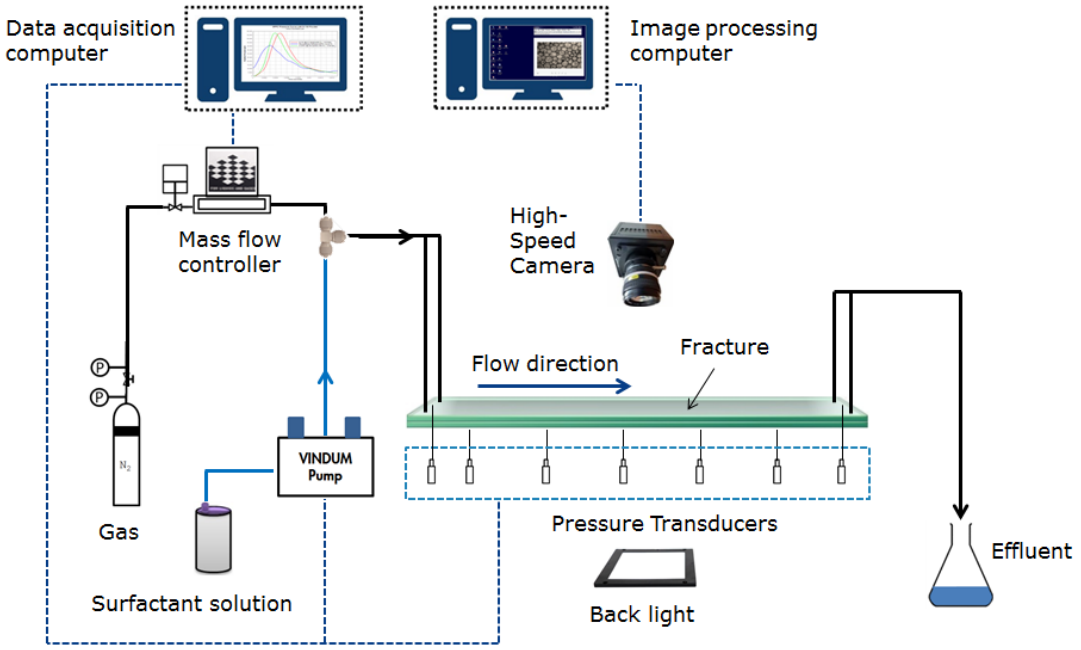

Figure 1 *Experimental setup.*

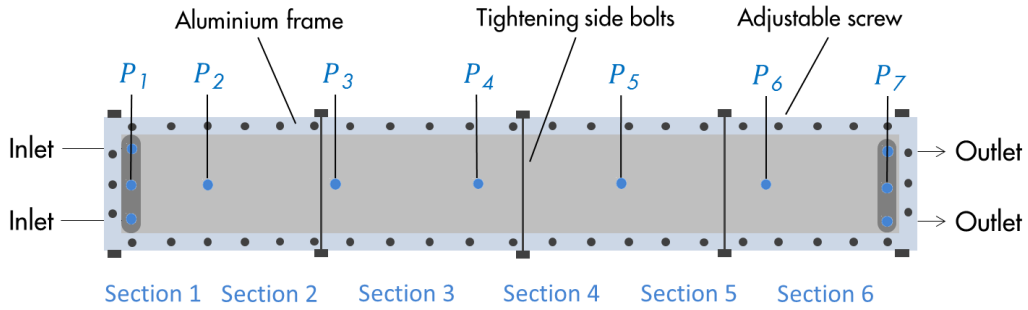

Figure 2 *Top view of a model fracture.*

Methodologies

In total seven sets of quality-scan experiments have been conducted in this study, as summarised in table 1. Superficial velocity is 1 mm/s for all experiments. Experiments are carried out on all three models by placing the model either horizontally or on its side. In quality-scan 1, foam is created inside model A by co-injecting gas and surfactant solution. In other quality-scan experiments, foam is pre-generated through a mixing Tees installed upstream the model fractures.

Seven pressure transducers are used to record pressure data during experiments. The steady-state pressure data are used to calculate the apparent viscosity to quantify the strength of steady-state foam. Apparent viscosity, μ_{app}, is calculated using the equation for laminar Newtonian flow in the slit (Witherspoon et al., 1980), as follows,

$$\mu_{app} = \frac{1}{12}\frac{1}{Q}\,|\nabla P|\,w\,d_H^3\,,$$

where Q is the total flow rate, ∇P is the pressure gradient of foam, w is the width of the model fracture, and d_H is the hydraulic aperture, the effective aperture determined from flow of water through the same model.

To analyse foam texture, bubble density (bubble number per 1 cm^2 of image), bubble size (bubble volume in units of x 10^{-2} mm^3), lamella length (in the unit of cm/cm^2 of image) and foam dryness (gas saturation), etc., are calculated from images of foam taken during experiments. The image analysis work in this study is done using ImageJ software.

No.	Fracture	Fracture hydraulic aperture, μ m	Fracture placement	Flow flow path	Foam generation strategy
1	Model A	78	Flat	Horizontal flow	Co-injection
2			Flat	Horizontal flow	Pre-generating foam
3			On its side	Sideways flow	Pre-generating foam
4	Model B	98	Flat	Horizontal flow	Pre-generating foam
5			On its side	Sideways flow	Pre-generating foam
6	Model C	128	Flat	Horizontal flow	Pre-generating foam
7			On its side	Sideways flow	Pre-generating foam

Table 1 *Summary of quality-scan experiments conducted in this study.*

Results

In horizontal-flow quality-scan experiments 1 and 2, stable foam is created at all tested foam qualities f_g (i.e. gas fractional flow). Bubble density, μ_{app} of foam and bubble size of steady-state foam along fracture at f_g of 0.8 are shown in Figure 3.

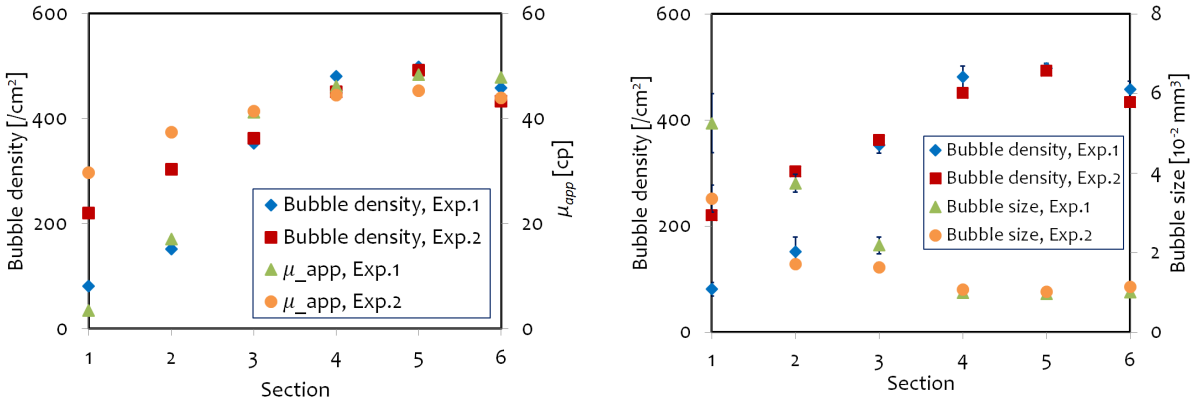

Figure 3 Left: *Bubble density and apparent viscosity of foam along model fracture;* ***Right:*** *Bubble density and bubble size of foam along model fracture. (See Figure 2 for definitions of model sections.) Results shown are based on f_g = 0.8 in quality-scan experiments on model A.*

According to Figure 3 left, foam bubble density correlates with foam strength well. Foam apparent viscosity increases as bubble density increases along the fracture. It is noteworthy that foam is stronger near the entry of the fracture when pre-generated foam is injected, compared to co-injection of gas and surfactant solution. Both pre-generated foam and in-situ-generated foam are refined along the fracture. Bubble density reaches its maximum at 459 bubbles/cm^2 in the second half of the fracture (i.e. sections 4, 5 and 6), where apparent viscosity reaches about 45 cp. Bubble size, shown in Figure 3 right, correlates inversely with bubble density. Foam bubbles are refined and have an average size of 1.1 x 10^{-2} mm^3 in the second half of the fracture.

It is concluded that stable foam is created in model A. The rough fracture surface provides sufficient generation sites to create foam bubbles in sections near the entry. In the second half of the fracture, the foam reaches Local Equilibrium (LE): the rate of foam lamella creation is equal to the rate of destruction, hence maintaining a stable foam.

Figure 4 shows comparison of horizontal-foam-flow experiment results on three models at f_g = 0.8. All data are LE average values in the second half of the fractures. According to Figure 4 left, bubble density decreases and bubble size increases as aperture of fracture increases. In Figure 4 right, when aperture increases, total lamella length per 1 cm^2 of image decreases. As a result, the drag force on lamella during foam flow decreases, yielding a lower viscous pressure gradient of foam in the fracture. Foam gets weaker as hydraulic aperture of fractures becomes larger. It is inferred that fractures with larger d_H have less capability to divert gas into matrix.

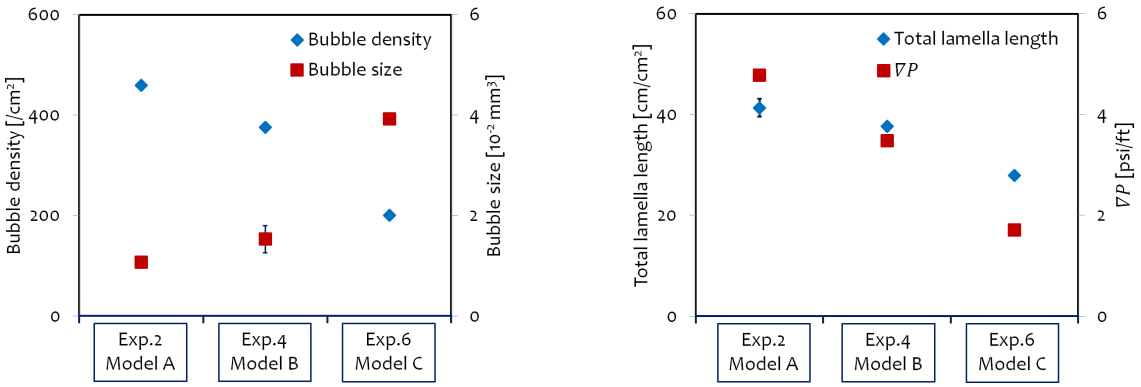

Figure 4 Left: *Bubble density and bubble size of foam on three models;* ***Right:*** *Total lamella length and pressure gradient of foam on three models. Results shown are based on LE average values.*

Figure 5 shows average LE gas saturation of foam in sideways-foam-flow experiments at different heights of three fractures at f_g = 0.8. Gas saturation is 9%, 18% and 27% greater at the top than the bottom for model A, B and C, respectively. For all three models, drier foam propagates along the top part of the fractures and wetter foam along the bottom. As a result, there are a gas-rich regime at the top of the fracture and a liquid-rich regime at the bottom. As aperture increases, the effect of gravity is more pronounced, and the regimes segregate more.

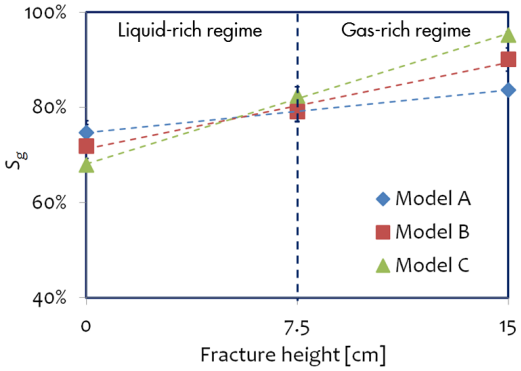

Figure 5 *Gas saturation of foam at different heights of the model fracture, with foam quality at 0.8.*

Conclusions

In this study, we conclude that the application of foam in vertical natural fractures (meters tall and tens of meter long) with an aperture up to hundreds of microns is problematic. Gravity segregation of phases in the foam in our experiments disables its capacity to divert gas flow from a tall fracture like our model into the matrix. As a result, there is a gas-rich regime at the top of the fracture and a liquid-rich regime at the bottom. The regimes segregate more as the aperture increases.

References

Kovscek, A. R., Tretheway, D. C., Persoff, P., & Radke, C. J. [1995] Foam flow through a transparent rough-walled rock fracture. *Journal of Petroleum Science and Engineering*, 13(2), 75-86.

AlQuaimi, B. I., & Rossen, W. R. [2019] Study of foam generation and propagation in fully characterized physical-model fracture. *Journal of Petroleum Science and Engineering*, 175, 1169-1181.

Farajzadeh, R., Wassing, B. M., & Boerrigter, P. M. [2012] Foam assisted gas–oil gravity drainage in naturally-fractured reservoirs. *Journal of Petroleum Science and Engineering*, 94, 112-122.

Witherspoon, P. A., Wang, J. S., Iwai, K., & Gale, J. E. [1980] Validity of cubic law for fluid flow in a deformable rock fracture. *Water resources research*, 16(6), 1016-1024.